

# Miniaturized High Split Ratio Bailey Power Divider Based on Multi-Ring Split Ring Resonators

Omar J. Jibreel<sup>1</sup>, Nihad I. Dib<sup>1</sup>, and Khair A. Shamaileh<sup>2</sup>

<sup>1</sup>Department of Electrical Engineering  
Jordan University of Science and Technology, Irbid, 22110, Jordan  
omar.j.jibreel@hotmail.com, nihad@just.edu.jo

<sup>2</sup>Department of Electrical and Computer Engineering  
Purdue University Northwest Hammond Campus, IN 46323, USA  
kalshama@pnw.edu

**Abstract**— In this paper, a miniaturized microstrip-based Bailey power divider is proposed by incorporating split ring resonators. New analytical design equations are derived for predefined power split ratios. To validate the proposed design methodology, two miniaturized dividers with 5:1 and 20:1 split ratios at 600 MHz are simulated, fabricated and measured. Simulated and measured results agree very well and show input port matching better than -15 dB and -20 dB at the design frequency, for the 5:1 and 20:1 dividers, respectively. The desired high split ratios are achieved with transmission parameters,  $S_{21}$  and  $S_{31}$ , of  $-1.9 \pm 0.1$  dB and  $-8.9 \pm 0.5$  dB for the 5:1 divider, and  $-0.9 \pm 0.1$  dB and  $-13.9 \pm 1.5$  dB for the 20:1 divider, respectively. Furthermore, a size reduction better than 65% is achieved as compared to conventional footprints.

**Index Terms**— Bailey power divider, high split ratio power dividers, miniaturization, split ring resonators, slow wave effect.

## I. INTRODUCTION

Power dividers find many applications in modern wireless communications systems, such as antenna feeders, radars, and amplifiers. Consequently, power dividers with enhanced electrical properties (e.g., high power-split ratio, multi-band operation) and physical characteristics (e.g., compact circuitry, ease of fabrication complexity/cost) are of utmost importance. To split power unequally at the output ports of a divider built with microstrip technology, a combination of printed circuit board (PCB) lines of high and low impedances are used. However, the design of high-split ratio dividers usually imposes microstrip lines with impractical widths. T-junctions, Wilkinson power dividers (WPDs), and Bagley power dividers (BPDs) are commonly utilized dividers for power division. A less known one, yet an attractive substitute, is the Bailey power divider [1].

The WPD uses lumped elements (i.e., resistors) to

improve output ports isolation. Nevertheless, high-split ratio WPDs require narrow lines. In [2], a new design method of an unequal WPD using arbitrary resistor value was presented, where line impedances were evaluated after the resistor value was arbitrarily chosen. In [3], a dual-band 1:10 WPD was designed by replacing the impractical high impedance line in the conventional design with cascaded dual band T-section structures based on derived analytical equations.

The BPD, which is usually used for equal splitting, suffers from several drawbacks, such as its large size, inconvenient ports arrangement, and unmatched output ports. In [4], T- and  $\pi$ -shaped networks were utilized to design compact dual-band unequal-split BPDs.

Unlike other dividers, when high ratios of splitting are of interest, the Bailey power divider does not require lines with impractical high characteristic impedances. Unequal splitting with different ratios using this divider can be easily obtained by only varying the input port position according to an analytical design equation. The main drawback of this divider, however, is its large physical area. Recently, many miniaturization techniques have been introduced to overcome the large area occupied by transmission lines [5-9]. In [10], stepped impedance sections were used to minimize the length of the quarter-wave arms of a coupler, which is an integral part in the Bailey power divider. In [11], the low impedance line, with high width, was substituted by equivalent parallel high impedance lines, while avoiding the impractical thin lines. In [12], the reduction was achieved by using T- and  $\pi$ -sections.

Split ring resonators (SRRs) are widely used to reduce the size of microwave components. In [13], two rose-shaped resonators were etched under every line in a hybrid quadrature coupler, and an algorithm to modify the width of the lines to compensate the effect of these resonators was presented. In [14], a hybrid branch line coupler was miniaturized by loading its lines with

square-split ring resonators. In this work, the effect of etching multi-ring SRRs is studied, and applied to the transmission lines (TLs) forming the Bailey power divider to achieve miniaturization.

The rest of this paper is organized as follows: In Section 2, the Bailey power divider is presented. In Section 3, the effect of etching SRRs with different number of rings is studied and applied to a hybrid quadrature coupler. Measurements and simulation results of a Bailey power divider loaded with SRRs are introduced in Section 4. Finally, conclusions are given in Section 5.

### II. BAILEY POWER DIVIDER

The unequal-split Bailey power divider is mainly a hybrid quadrature line coupler excited at its two input ports with equal amplitudes but different phases. At the output ports, the output signals are the superposition of two input signals fed to a hybrid coupler. The signals combine at the output ports such that the output amplitude ratio can be any desired value, while maintaining an in-phase relationship at the output [1]. To excite the two input ports of the hybrid coupler, a simple T-junction with unequal line lengths is connected to the inputs to produce the required phase difference, as illustrated in Fig. 1.

At the design frequency,  $b = \lambda/4$ , where  $\lambda$  is the wavelength. The power ratio at the output ports of the splitter is given as:

$$P_3 / P_2 = \tan^2(\pi a / 2b). \tag{1}$$

Therefore, the power split-ratio (at the design frequency) is simply determined by the position of the input port (i.e. the ratio  $a/b$ ).

Figure 2 shows the layout of 600 MHz equal-split Bailey power divider ( $a/b = 1/2$ ) using a 1.5 mm-thick FR-4 substrate with a dielectric constant of 4.4. As can be noticed, the divider occupies a very large area. A miniaturization technique, using SRRs will be discussed in the following section, and applied to reduce the Bailey power divider area.

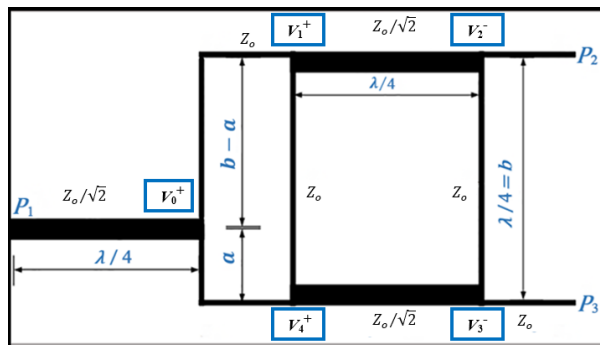


Fig. 1. Layout of the conventional Bailey power divider.

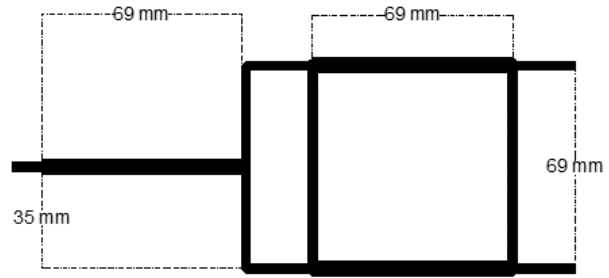


Fig. 2. Layout of 600 MHz equal-split Bailey power divider.

### III. SPLIT RING RESONATORS

Meta-materials are synthesized materials, in which, electron oscillations over electrically small inclusions can result in new electromagnetic properties. SRRs are artificial magnetic metamaterials (AMMs). A conventional single split ring resonator cell has a pair of enclosed loops with splits at opposite ends. Etching an AMM in the ground plane under a microstrip TL generates a high magnetic coupling between the line and the rings. The SRR cell has a resonance (i.e., stopband) frequency that depends on its dimensions [15]. Loading a TL with an SRR causes a Slow Wave Effect, where the loaded TL has the properties of a longer one, which can be exploited to reduce the size of microwave components formed by these TLs.

#### A. Slow-wave effect

A schematic diagram of a microstrip TL loaded with an electrically small 2-ring resonator etched in the ground plane is presented in Fig. 3. The resonance frequency and the effect of this resonator on the TL depend on its dimensions and number of rings. Adding another cell with the same resonance frequency will increase the effect on the TL. As the radius of the etched resonator increases, its stopband frequency decreases. A fine tuning can be also obtained by changing the width of the rings and the gaps between them.

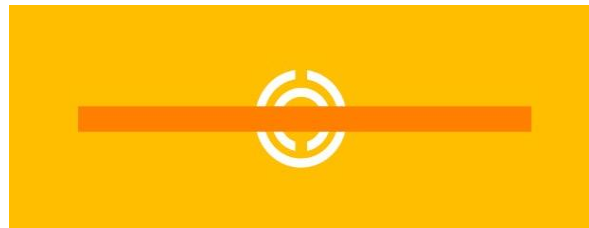


Fig. 3. Microstrip TL loaded with a two-ring SRR.

A 50 Ω microstrip TL is designed to exhibit a 90° phase shift at 600 MHz in the absence of the resonator. Different resonators with different stopband frequencies are loaded to the TL, and more rings are added inside

these resonators to study their effect on the line. Figure 4 illustrates a 4-ring SRR. The dimensions of the used SRRs are indicated in Table 1 considering the previously mentioned FR-4 substrate.

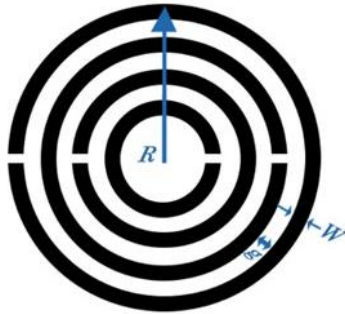


Fig. 4. 4-ring SRR.

Table 1: SRRs dimensions and their corresponding stopband frequencies

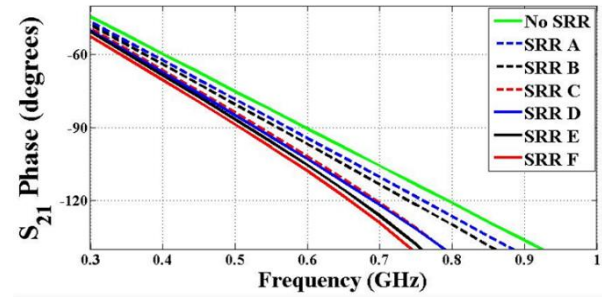
SRR	Rings	R (mm)	W (mm)	g (mm)	Stopband Frequency (GHz)
A	2	5.5	0.15	0.20	1.8
B	2	7.5	0.25	0.25	1.4
C	4	7.5	0.25	0.25	1.1
D	2	8.5	0.50	0.50	1.1
E	4	8.5	0.50	0.50	1.0
F	8	8.5	0.50	0.50	0.9

Table 1 shows the relation between the resonators dimensions and their stopband frequencies obtained through full-wave simulation. As the number of the rings increases, the resonance frequency decreases. SRRs C and D have the same resonance frequency, even though they have different dimensions. The extra rings and the narrow rings width in SRR C compensated the greater radius of SRR D. This fact can be taken into consideration to avoid the large area that may be occupied by the resonator when lower stopband frequencies are desired.

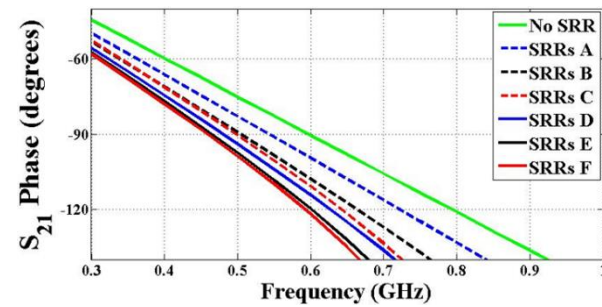
The slow-wave effect caused by these resonators can be determined by examining the transmission parameter phase [13]. Figure 5 (a) shows the phase of  $S_{21}$  for the microstrip lines with the resonators in Table 1 etched in the ground plane. For the unloaded TL, a  $90^\circ$  shift occurs at the design frequency 600 MHz. However, for the loaded lines, the  $90^\circ$  phase shift occurs at lower frequencies. This implies that the loaded line performs as a longer one and can be shortened. As the resonance frequency of the etched SRR decreases, the slow-wave effect on the loaded line increases, as shown in Fig. 5 (a).

For further shortening, two cells can be etched under the same line. The results of adding an extra cell are illustrated in Fig. 5 (b). The transmission parameter of the designed line has a phase of  $90^\circ$  at

0.46 GHz when two cells of SRR F are applied. In other words, the resulting line has the electrical parameters of a conventional 91 mm length line, while its actual length is 68 mm.



(a)



(b)

Fig. 5. The slow-wave effect using: (a) a single cell SRR, and (b) two cells SRRs.

The factor by which the line can be shortened is initially calculated by [13]:

$$F = -\phi / 90^\circ, \tag{2}$$

where  $\phi$  is the phase of  $S_{21}$  (in degrees) at the design frequency after loading the resonators. The length can be then tuned to achieve the desired transmission properties.

### B. Hybrid coupler with SRRs

Firstly, SRRs are applied to a hybrid coupler with a design frequency of 600 MHz, as it is the main part of the Bailey power divider. Two 8-ring SRRs (with dimensions of SRR F in Table 1) are etched under each TL in the coupler, then, the line is shortened to obtain the same transmission properties of the original one. The layout of the loaded coupler is shown in Fig. 6.

The coupler in Figure 6 has an area of  $17.5 \text{ cm}^2$  as compared to  $47.6 \text{ cm}^2$  occupied by the conventional design. In Fig. 7, the simulated scattering parameters of the reduced size coupler show that it operates properly at the design frequency, with input port matching better than  $-35 \text{ dB}$  and isolation parameters better than  $-20 \text{ dB}$ . The transmission parameters,  $S_{21}$  and  $S_{31}$ , are in close proximity to  $-3 \text{ dB}$ .

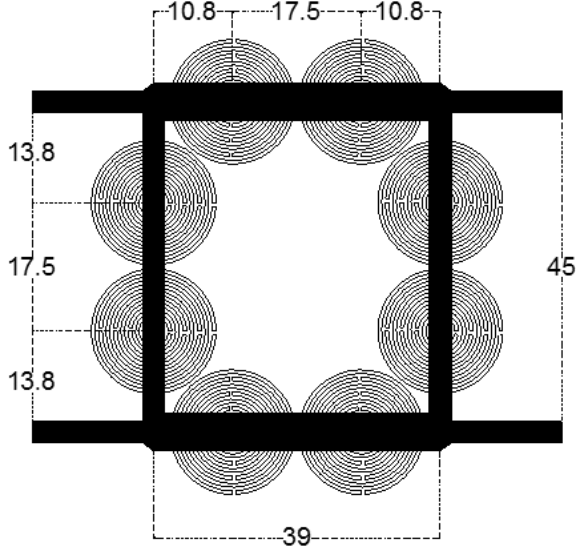


Fig. 6. Hybrid coupler loaded with 8-ring SRRs (dimensions in mm).

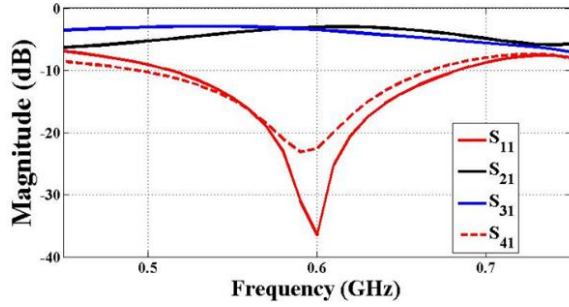


Fig. 7. Simulated  $S$ -parameters of the miniaturized coupler using SRRs.

#### IV. MINIATURIZED BAILEY POWER DIVIDER

##### A. New formulation

As the arms of the SRR-loaded coupler in the Bailey power divider are shortened, the expression in (1) cannot be used. In this subsection, a new formulation based on the miniaturized coupler is derived. Figure 8 represents the layout of a reduced size Bailey power divider.

The lengths  $x$  and  $y$  need to be calculated to achieve a specific splitting ratio. The design equation is derived based on transmission line theory. Referring to Fig. 8, at the design frequency, the incident voltage waves at the input ports of the coupler are given as follows:

$$V_1^+ = V_o^+ e^{-j\beta x}, \quad (3a)$$

$$V_4^+ = V_o^+ e^{-j\beta y}, \quad (3b)$$

where  $\beta = 2\pi/\lambda$  at the design frequency. The scattered voltages at the output ports of the coupler can be calculated as the superposition of the response of a hybrid coupler to two input signals, as follows:

$$V_2^- = j \frac{V_1^+}{\sqrt{2}} + \frac{V_4^+}{\sqrt{2}}, \quad (4a)$$

$$V_3^- = j \frac{V_4^+}{\sqrt{2}} + \frac{V_1^+}{\sqrt{2}}. \quad (4b)$$

After some mathematical manipulations, one can derive the following expressions for the magnitudes of the output voltages:

$$|V_2^-| = |V_o^+| [1 + \sin \beta(x - y)]^{1/2}, \quad (5a)$$

$$|V_3^-| = |V_o^+| [1 - \sin \beta(x - y)]^{1/2}. \quad (5b)$$

The power at the output ports can be written as follows:

$$P_2^- = \frac{|V_2^-|^2}{2Z_o} = \frac{|V_o^+|^2}{2Z_o} [1 + \sin \beta(x - y)], \quad (6a)$$

$$P_3^- = \frac{|V_3^-|^2}{2Z_o} = \frac{|V_o^+|^2}{2Z_o} [1 - \sin \beta(x - y)]. \quad (6b)$$

Thus, the design equation of the miniaturized Bailey power divider, with a split ratio of  $R = P_3^-/P_2^-$  is:

$$R = \frac{[1 + \sin \beta(x - y)]}{[1 - \sin \beta(x - y)]}. \quad (7)$$

Equation (7) shows that the split ratio depends on the difference between the lengths of the two arms feeding the coupler. It also applies to the conventional design where (1) is a special case when  $x + y = \lambda/4$ .

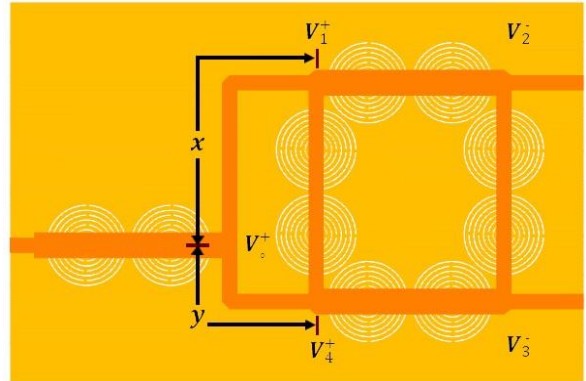


Fig. 8. Layout of the reduced size Bailey power divider.

##### B. Experimental results

Figure 9 shows the layout of a 5:1 ( $P_2 : P_3 = 5 : 1$ ) SRR-loaded 600 MHz Bailey divider. Using equation (7), the difference between the two arms should be  $0.116 \lambda$  at 600 MHz (33 mm), and tuned to be 34 mm. The input arm of the divider is also shortened by etching two 8-ring SRRs. The designed divider is fabricated on the previously mentioned FR-4 substrate. The  $S$ -parameters are measured using an E5071C ENA Keysight vector network analyzer and compared with the



simulated ones in Fig. 10, which shows measured input port matching better than -15 dB. The transmission parameters,  $S_{21}$  and  $S_{31}$ , are measured to be -1.9 dB and -8.3 dB, at the design frequency, respectively. Such values are close to the theoretical calculations, -0.8 dB and -7.8 dB, respectively.

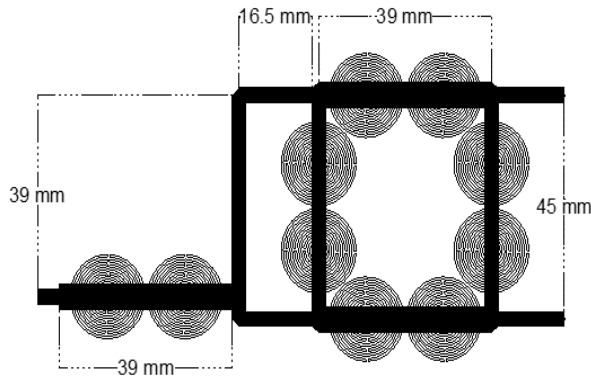


Fig. 9. Layout of the 5:1 miniaturized Bailey power divider.

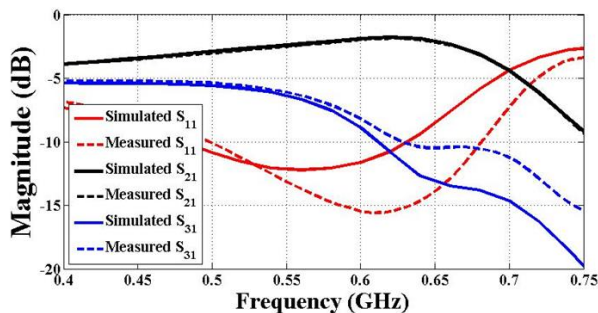


Fig. 10. Simulated and measured results of the miniaturized 5:1 Bailey power divider.

Instead of using SRRs at the input arm, it can be meandered as shown in Fig. 11. The input arm is positioned to obtain a 20:1 split ratio. The difference between the coupler feeders is  $0.18 \lambda$  at 600 MHz (49.3 mm). Measured and simulated results are shown in Fig. 12. The measured input port matching is better than -20 dB at the design frequency. Simulated transmission parameters,  $S_{21}$  and  $S_{31}$ , are -0.9 dB and -13.9 dB, respectively, which are in a good agreement with the theoretical values, -0.2 dB and -13.2 dB, respectively. The small discrepancies between the simulated and measured results are thought to be due to conductor losses, and the soldering of the connectors to the lines.

A photograph of one of the fabricated dividers is illustrated in Fig. 13. The SRRs are etched in the ground plane exactly under the coupler TLs. The fabricated divider has an area of around 35% of the one occupied by the conventional divider.

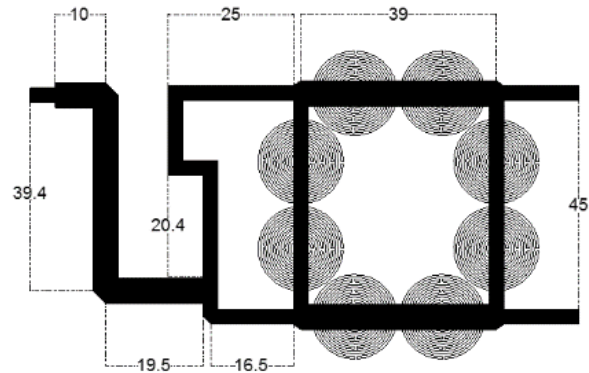


Fig. 11. The fabricated 20:1 miniaturized Bailey power divider (dimensions in mm).

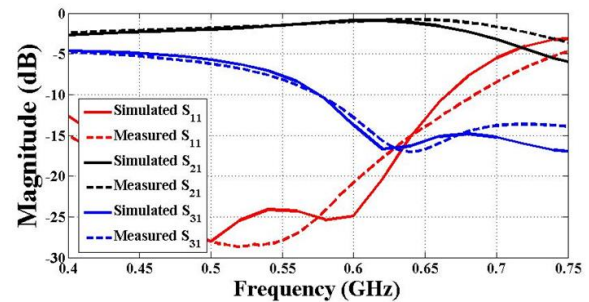


Fig. 12. Simulated and measured results of the miniaturized 20:1 Bailey power divider.

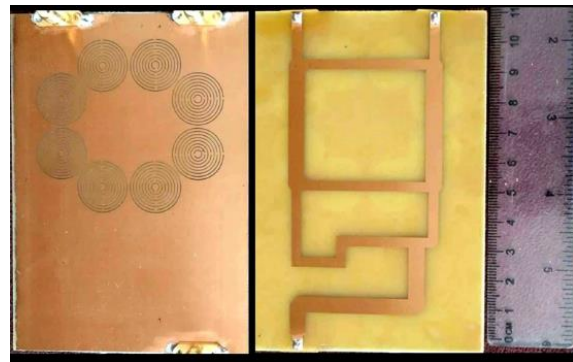


Fig. 13. Photograph of the fabricated 20:1 Bailey power divider with SRRs.

## V. CONCLUSION

In this paper, the Bailey power divider was presented as a high split ratio divider which tackles the problem of the high impedance thin lines problem. A size reduction technique based on SRRs was studied, where the slow-wave effect resulting by these resonators was utilized to shorten the microstrip transmission lines. Adding more rings inside the resonators increased the slow-wave effect allowing for further size reduction. The

miniaturization technique was applied to reduce the large size of the Bailey power divider. Two prototypes of the miniaturized divider were fabricated and tested. High splitting ratios of 5:1 and 20:1 were achieved. The fabricated dividers have an area of less than 35% of the one occupied by the conventional 600 MHz Bailey power divider.

### ACKNOWLEDGMENT

The authors acknowledge the financial support of the Deanship of Scientific Research at the Jordan University of Science and Technology under research grant number 2017/331.

### REFERENCES

- [1] M. C. Bailey, "A simple stripline design for uneven power split," *NASA Technical Memorandum* (81870), 1980.
- [2] D. Lee, H. Doo, Y. Jang, H. Kim, S. Han, J. Lim, K. Choi, and D. Ahn, "A new design method of the unequal Wilkinson power divider using an arbitrary resistor value," *Microwave and Optical Technology Letters*, vol. 58, no. 10, pp. 2450-2452, 2016.
- [3] K. Al-Shamaileh, N. Dib, and S. Abushamleh, "A dual-band 1:10 Wilkinson power divider based on multi-T-section characterization of high-impedance transmission lines," *IEEE Microwave and Wireless Components Letters*, vol. 27, no. 10, pp. 897-899, 2017.
- [4] O. Abu-Al-Nadi, *Analysis and design of compact multi-frequency Bagley power dividers (Master's thesis)*, Department of Electrical Engineering, Jordan University of Science and Technology, Jordan, Irbid, 2012.
- [5] K. Al-Shamaileh, N. Dib, and A. Sheta, "Design of miniaturized unequal split Wilkinson power divider with harmonics suppression using non-uniform transmission lines," *Applied Computational Electromagnetics Society (ACES) Journal*, vol. 26, no. 6, pp. 530-538, June 2011.
- [6] M. Hayati, S. Roshani, and S. Roshani, "Miniaturized Wilkinson power divider with nth harmonic suppression using front coupled tapered CMRC," *Applied Computational Electromagnetics Society (ACES) Journal*, vol. 28, no. 3, pp. 221-227, Mar. 2013.
- [7] D. Hawatmeh, K. Al-Shamaileh, and N. Dib, "Design and analysis of multi-frequency unequal-split Wilkinson power divider using non-uniform transmission lines," *Applied Computational Electromagnetics Society (ACES) Journal*, vol. 27, no. 3, pp. 248-255, Mar. 2012.
- [8] G. Wu, G. Wang, L. Hu, Y. Wang, and C. Liu, "A miniaturized triple-band branch line coupler based on simplified dual-composite right/left-handed transmission line," *Progress in Electromagnetics Research C*, vol. 39, pp. 1-10, 2013.
- [9] D. Ji, B. Wu, X. Ma, and J. Chen, "A compact dual-band planar branch-line coupler," *Progress in Electromagnetics Research C*, vol. 32, pp. 43-52, 2012.
- [10] C. Hsu, C. Chang, and J. Kuo, "Design of dual-band microstrip rat race coupler with circuit miniaturization," *IEEE/MTT-S International Microwave Symposium*, Honolulu, HI, pp. 177-180, July 2007.
- [11] S. Karthikeyan and R. Kshetrimayum, "Extremely unequal Wilkinson power divider with dual transmission lines," *Electronic Letters*, vol. 46, no. 1, pp. 90-91, 2010.
- [12] M. Alkanhal and A. Mohra, "Dual-band ring couplers using T and Pi sections," *International Journal of Microwave and Optical Technology*, vol. 3, no. 4, pp. 460-466, 2008.
- [13] B. Savitri, V. Fono, B. Alavikia, L. Talbi, and K. Hettak, "Novel approach in design of miniaturized passive microwave circuit components using metamaterials," *Microwave and Optical Technology Letters*, vol. 59, no. 6, pp. 1341-1347, 2017.
- [14] L. Al-Khateeb, "Miniaturized hybrid branch line couplers based on square-split resonator loading technique," *Progress in Electromagnetics Research Letters*, vol. 40, pp. 153-162, 2013.
- [15] J. Pendry, A. Holden, D. Ribbins, and W. Stewart, "Magnetism from conductors and enhanced non-linear phenomena," *IEEE Trans. Microwave Theory Tech.*, vol. 47, no. 11, pp. 2075-2084, 1999.